LCLS-TN-01-1
November 14,2001

X-Band RF Harmonic Compensation for Linear Bunch Compression in the LCLS

Paul Emma
SLAC
November 14, 2001

ABSTRACT

An X-band 4th harmonic RF section is used to linearize the bunch compression process in the Linac Coherent Light Source [1]. The optimum voltage is calculated to compensate both for the second-order RF time-curvature, and for the second-order momentum compaction terms. This compensated compression retains, to a much higher degree, the initial temporal distribution of the bunch, reducing the effects of coherent synchrotron radiation [2], and also reduces the sensitivity of the final compression to bunch arrival time variations.

1 Introduction

The process of electron bunch compression is usually described as a linear transformation of the longitudinal phase space which reduces bunch length while increasing energy spread. For future FEL's, such as described in [1] and [3], the final compression is so extreme as to be easily dominated by non-linear effects such as sinusoidal RF time-curvature and the compressor's second-order path-length dependence on particle energy. For simple magnetic chicanes and the like, which are ubiquitous in future FEL's, the RF and path-length effects always conspire with the same signed second-order terms to make the problem worse. With increased compression, very sharp temporal spikes can be generated which may drive unwanted collective effects such as coherent synchrotron radiation (CSR) and longitudinal wakefields in an undulator. The CSR effect and its rapid amplification with non-linear compression is highlighted in reference [2].

This note describes the use of a short section of radio frequency accelerating fields at a higher harmonic, with respect to the main accelerating linac RF, to compensate the compression transformation up to second order, thereby maintaining the initial temporal bunch profile and avoiding unnecessary amplification of undesired collective effects. By linearizing the net transformation, the level of final compression is also made much less sensitive to bunch arrival time errors (timing jitter). Similar schemes have been proposed at Boeing [4] and at DESY [5].

2 Second-Order Compression Effects

For generality, we assume here that the electron bunch is passed through two linac segments: 1) a near-crest phased injector, and 2) an off-crest phased pre-compression correlation linac as shown in **Figure 1**. The symbols used for voltage (V_i), RF wavelength (λ_s and λ_x), and phase (φ_i) of each section, as well as the chicane momentum compaction coefficients (R_{56} and T_{566}) are defined in the figure.

With initial energy E_i, and after passage through the three RF systems, the electron energy (charge e) at the chicane is

$$E_0 \approx E_i + eV_0\cos(\varphi_0 + k_s z_0) + eV_1\cos(\varphi_1 + k_s z_0) + eV_x\cos(\varphi_x + k_x z_0), \qquad (1)$$

where $k_{s,x}$ ($\equiv 2\pi/\lambda_{s,x}$) is the RF wavenumber, z_0 is the longitudinal position of the electron with respect to the reference particle (bunch center), and the bunch head is at $z_0<0$. The RF phase, φ, is defined to be zero at accelerating crest and a phase in the interval ($-90° < \varphi < 0$) will accelerate the bunch head less than it will the bunch tail.

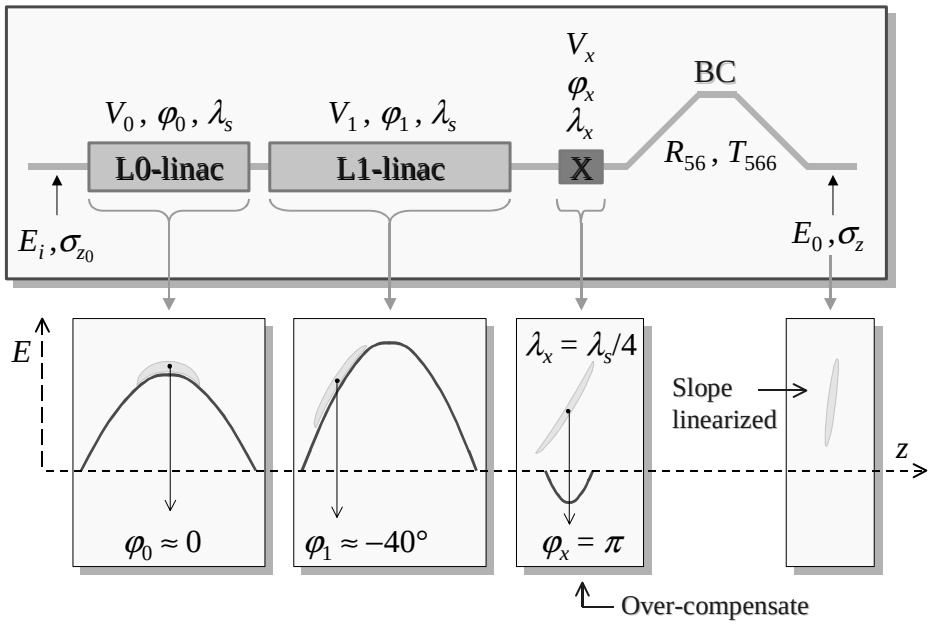

Figure 1. Schematic of two linac segments followed by harmonic RF and compressor chicane. The bunch is compressed from an initial rms length σ_{z_0} to a final length σ_z with initial energy E_i and final energy E_0 (bunch head at left: $z<0$).

For 2nd-order harmonic compensation, the X-band RF phase is set to $\varphi_x = \pm\pi$ ($eV_x \geq 0$), at decelerating crest and the relative energy deviation with respect to the reference particle, to second-order in bunch length coordinate z_0, is then given by

$$\Delta E/E_0 \approx \left(\frac{-eV_0 k_s \sin\varphi_0 - eV_1 k_s \sin\varphi_1}{E_0}\right)\cdot z_0 + \left(\frac{-eV_0 k_s^2 \cos\varphi_0 - eV_1 k_s^2 \cos\varphi_1 + eV_x k_x^2}{2E_0}\right)\cdot z_0^2 . \quad (2)$$

The incoming uncorrelated energy spread is ignored here for simplicity, but does not change the arguments below. Equation (2), the relative energy deviation, is abbreviated

$$\Delta E/E_0 \approx a z_0 + b z_0^2 , \quad (3)$$

where $a>0$ for $eV_0>0$, $eV_1>0$, ($-90° < \varphi_0 \leq 0$), and ($-90° < \varphi_1 < 0$). Similarly, $b<0$ with the harmonic RF switched off ($eV_x = 0$).

The compressor chicane transforms energy deviation to path-length deviation, z, and is used to finally compress the energy 'chirped' bunch. The bunch length coordinate transformation, to second order, is

$$z = z_0 + R_{56}\cdot(\Delta E/E_0) + T_{566}\cdot(\Delta E/E_0)^2 , \quad (4)$$

where for a typical chicane, the two coefficients are approximately related by $T_{566} \approx -3R_{56}/2$. Equation (3) is then substituted into Eq. (4) and the compression transformation is written to second order as

$$z = (1 + aR_{56}) \cdot z_0 + \left(bR_{56} + a^2 T_{566}\right) \cdot z_0^2 , \tag{5}$$

with the coefficients a and b taken from Eq. (2) as compared to Eq. (3). Again, the uncorrelated energy spread is ignored here for simplicity.

The first term in Eq. (5) defines the linear bunch compression and can be set to zero for full, linear compression by setting $R_{56} = -1/a < 0$. In this case the final bunch length will be determined by the non-linear terms and the uncorrelated energy spread. To linearize the transformation, the second term must be set to zero.

$$bR_{56} + a^2 T_{566} = 0 \tag{6}$$

In the case of chicane (or wiggler) compression using *accelerating* RF, and the definition with bunch head at $z<0$, then $b<0$, $R_{56}<0$, and $T_{566}>0$, and the two contributions to this non-linearity (RF and T_{566}) always add making Eq. (6) impossible to realize. A non-chicane system might be used to flip the sign of R_{56} (>0) and therefore use an RF phase in the positive interval ($0 < \varphi_1 < +90°$). This flips the sign of a without flipping b and since T_{566} is, for all practical systems, always >0, the two contributions in Eq. (6) might be made to cancel. This situation, however requires a much more complicated compressor system including quadrupole magnets, typically much more space, and possibly even sextupole compensation of transverse chromatic effects. Another possibility is to use a decelerating RF phase to flip the sign of b (*e.g.*, $eV_1<0$) [6]. For an FEL injector system at a few hundred MeV, however, this typically reduces the energy too much and may easily generate space charge emittance dilution. A more flexible way to realize Eq. (6) is to add a harmonic RF system with wavelength ratio $\lambda_s/\lambda_x = n$ (= 2,3,4,…).

3 Harmonic Compensation

With the harmonic RF section included, the second-order terms in the compression transformation can be cancelled by applying Eq. (6).

$$b = -\frac{T_{566}}{R_{56}} a^2 \approx \frac{3}{2} a^2 , \quad \text{or} \tag{7}$$

$$\frac{-eV_0 k_s^2 \cos\varphi_0 - eV_1 k_s^2 \cos\varphi_1 + eV_x k_x^2}{2E_0} = -\frac{T_{566}}{R_{56}} \left(\frac{-eV_0 k_s \sin\varphi_0 - eV_1 k_s \sin\varphi_1}{E_0} \right)^2 \tag{8}$$

Since the second-order effect is to be compensated, the RF phase of the harmonic section should be chosen at decelerating crest (see **Figure 1**). It is also possible to compensate third-order terms by including an off-crest harmonic RF phase [5]. Unfortunately, particle tracking through the injector indicate that the dominant third-order terms are generated soon after the RF photocathode gun by space-charge forces [7] and are of a sign that is difficult to cancel without also partially canceling the necessary linear compression terms, resulting in very inefficient acceleration.

At decelerating crest, the harmonic voltage also lowers the beam energy. Therefore it is necessary to increase the voltage of the main RF section, V_1. Holding the chicane energy constant at E_0 gives the main linac voltage V_1 as a function of the harmonic voltage V_x.

$$eV_1\cos\varphi_1 = E_0 - E_i - eV_0\cos\varphi_0 + eV_x \tag{9}$$

Similarly, the compression factor is also dependent on main RF voltage settings, so a second requirement is to hold the compression factor, a, constant.

$$eV_1\sin\varphi_1 = -eV_0\sin\varphi_0 - \frac{aE_0}{k_s} \tag{10}$$

The two constraints in Eqs. (9) and (10), of constant chicane energy and constant final bunch length, are used to calculate the harmonic voltage needed to completely cancel second-order compression terms by eliminating eV_1 terms from Eq. (7). The linear compression relation $-aR_{56} \approx (1 - \sigma_z/\sigma_{z_0})$ is also applied, which ignores the typically insignificant incoherent energy spread, and the necessary harmonic voltage is

$$eV_x = \frac{E_0\left\{1+\frac{1}{2\pi^2}\frac{\lambda_s^2 T_{566}}{|R_{56}|^3}\left(1-\sigma_z/\sigma_{z_0}\right)^2\right\} - E_i}{\left(\lambda_s/\lambda_x\right)^2 - 1}. \tag{11}$$

The square of the harmonic ratio $n^2 \equiv (\lambda_s/\lambda_x)^2$ in the denominator suggests that higher harmonics are more efficient for second-order compensation, decelerating the beam less. For an X-band harmonic (n = 4, $\nu_x \approx 11.424$ GHz), with S-band main RF ($\lambda_s \approx 105$ mm, $\nu_x \approx 2.856$ GHz), $R_{56} \approx -35.5$ mm $\approx -2T_{566}/3$, a compression ratio $\sigma_z/\sigma_{z_0} \approx 0.24$, injection energy 7 MeV, and final energy 250 MeV, the harmonic voltage required is 22 MV, which is also the deceleration in the X-band section. An X-band klystron with ~10-MW of power and a 0.6-m long structure are required. Both exist at SLAC. **Table 1** lists the parameters for both the X-band OFF and the X-band ON scenario. The X-band RF voltage is reduced from the 22-MV prediction of Eq. (11) to 18 MV due to wakefield effects of both the S-band and X-band RF structures. **Figure 2** shows a photograph of an existing 0.5-m long X-band RF section developed for the Next Linear Collider (NLC).

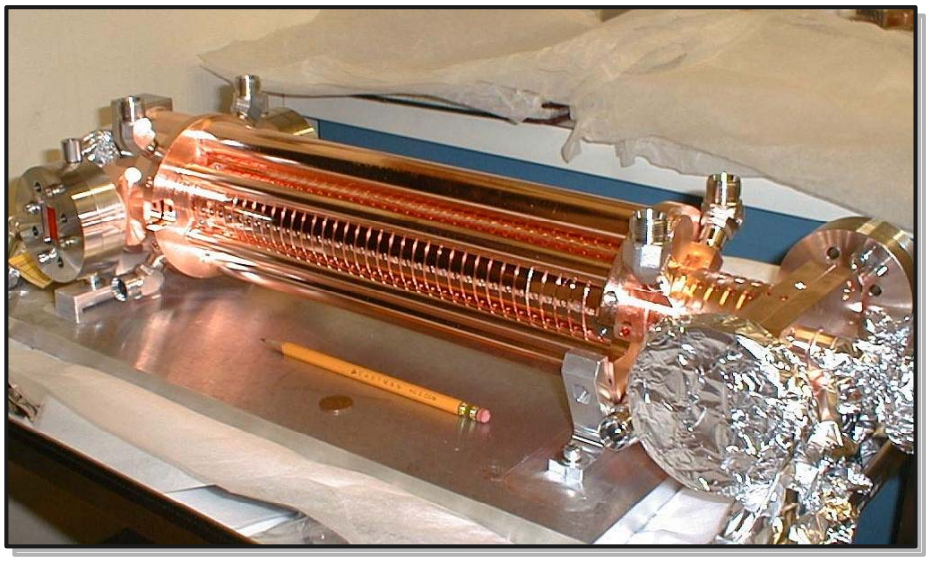

Figure 2. An X-band RF section with 0.5-m length developed for NLC R&D.

Table 1. Parameters for LCLS first compression stage with and without X-band harmonic compensation.

parameter	symbol	X-band OFF	X-band ON	units
Linac-1 S-band RF voltage	eV_1	138	153	MeV
Linac-1 S-band RF phase	φ_1	–43.1	–39.0	S-deg
Harmonic X-band RF voltage	eV_x	0	18	MeV
Harmonic X-band RF phase	φ_x	—	–180	X-deg
Injector S-band RF voltage	eV_0	144		MeV
Injector S-band RF phase	φ_0	–1.5		S-deg
Chicane momentum compaction	R_{56}	–35.5		mm
2nd-order momentum compaction	T_{566}	+53.2		mm
Injection energy at gun exit	E_i	7		MeV
Final energy at chicane	E_0	250		MeV
rms bunch length before chicane	σ_{z_0}	830		μm
rms bunch length after chicane	σ_z	200		μm
S-band RF wavelength	λ_s	105		mm
X-band RF wavelength	λ_x	26.2		mm

Figure 3 shows the simulated energy profile, longitudinal phase space, and temporal profile after the second S-band RF segment, but prior to the chicane, with the X-band RF switched off. The slight curvature in the energy-z correlation is mostly due to the sinusoidal character of the S-band RF. With parameters set to compress the bunch from 830 μm rms to 200 μm rms, but without the X-band RF harmonic compensation, a sharp peak current spike develops at the bunch head due to the combined RF and T_{566} non-

linearities (see **Figure 4**). The result is an extreme case which might destroy the transverse emittance due to amplified CSR effects.

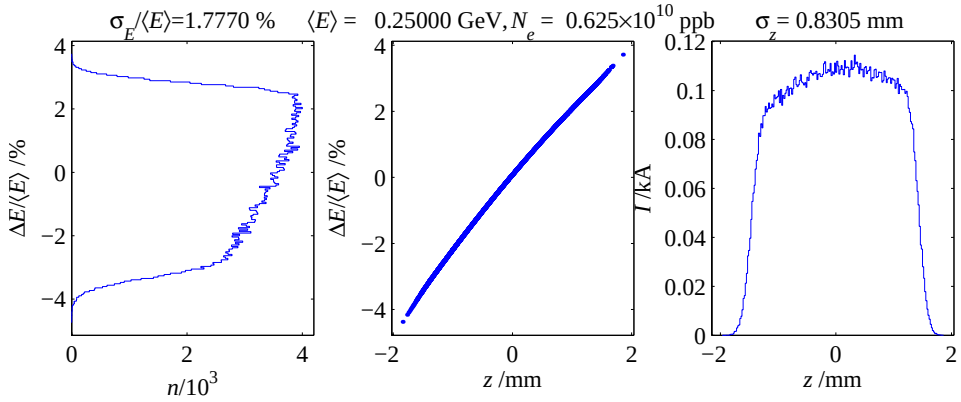

Figure 3. Energy profile (left), longitudinal phase space (center), and temporal profile (right) after second S-band RF segment, but prior to chicane, with X-band RF switched OFF (bunch head at left: z<0).

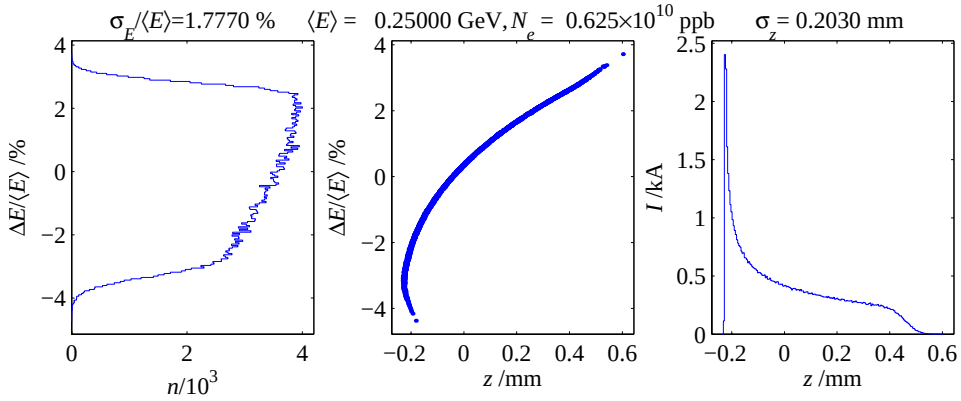

Figure 4. AFTER chicane, with X-band RF switched OFF. An undesirable sharp current spike develops at bunch head (z<0) due to the non-linear RF and chicane compression.

Figure 5 shows the phase space again after the second S-band segment, which is now re-adjusted in phase and voltage to retain the linear compression goal of 200 μm using Eqs. (9) and (10) (*i.e.*, the energy and energy spread at chicane entrance is held constant at 250 MeV and 1.77%, respectively). The energy is 268 MeV here so that the chicane energy, after X-band deceleration, will still be 250 MeV.

Figure 6 shows the phase space, now at 250 MeV, after the X-band section which is now switched on to 18 MV at decelerating crest phase. The energy-z correlation is slightly cupped which is now opposite of that in **Figure 5**. This is used to compensate the T_{566} effect in the upcoming chicane. The final phase space is shown in **Figure 7** after the chicane with the X-band RF on. The compressed temporal distribution is nearly unchanged with respect to the initial profile in **Figure 5**, except for the compression to

200 μm, while the energy-z correlation is very linear. Longitudinal wakefields of the S- and X-band RF structures are included here and add a less significant, but higher order non-linearity to the correlations which reduce the required X-band voltage to 18 MV.

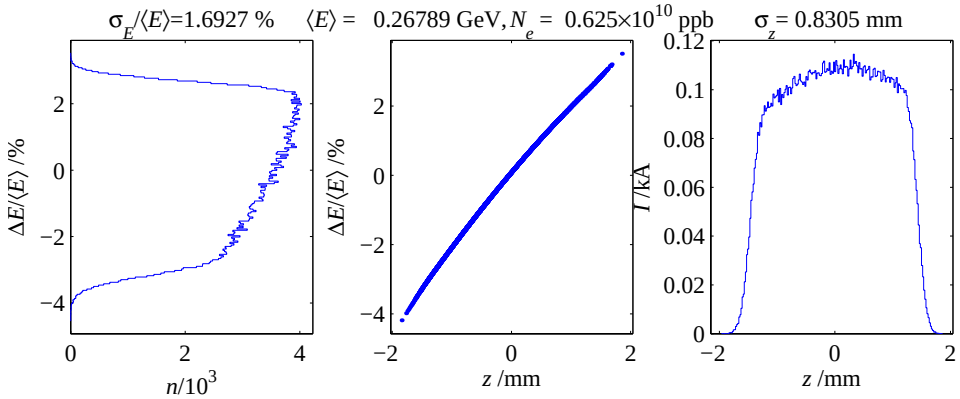

Figure 5. Phase space after second S-band RF segment which is readjusted in order to retain the linear compression goal of 200 μm at 250 MeV.

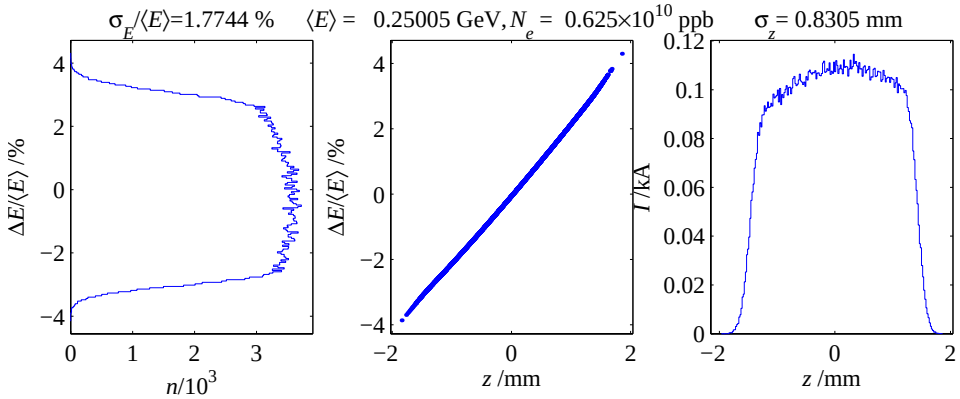

Figure 6. Phase space BEFORE chicane, but after X-band RF which is now switched ON at 18 MV. The energy-z correlation is slightly cupped here to compensate for the T_{566} term in the upcoming chicane.

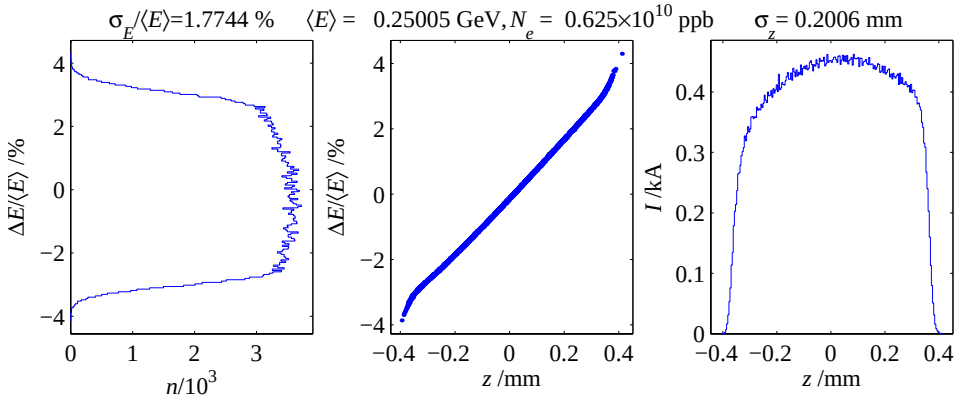

Figure 7. Phase space AFTER chicane, with X-band RF ON. The compressed temporal distribution at right is nearly unchanged with respect to the initial profile in **Figure 5**, except for the compression.

4 Time Jitter Sensitivity

The linear compression coefficient, a, is also sensitive to phase (timing) errors, as seen in Eq. (2). By linearizing the transformation, the harmonic compensation also maintains a more constant final compressed bunch length in the presence of bunch arrival-time errors, which may occur from pulse to pulse, and are measured with respect to the nominal RF phase. Such arrival-time errors are typically generated by the RF photocathode laser and are therefore common to all RF systems, S-band and X-band. **Figure 8** shows the compressed rms bunch length achieved as a function of bunch arrival-time error, Δt. The solid (red) line is with X-band RF OFF and dashed (blue) line is with X-band RF at 18 MV. The sensitivity is greatly reduced with X-band ON, but perfect compensation is not achieved due to the wakefield influence on the optimal X-band voltage setting. At 22 MV (not shown) perfect compensation is achieved but the temporal bunch profile begins to deviate from its initial profile.

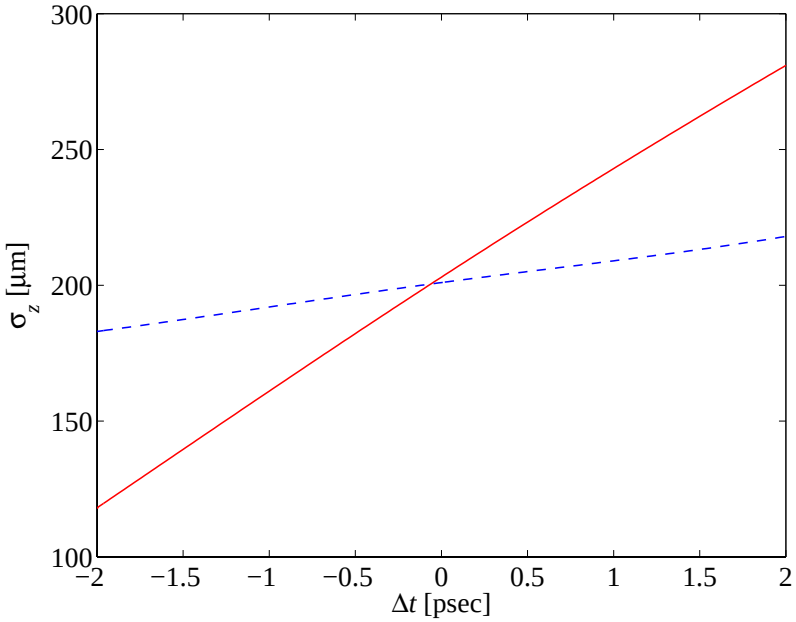

Figure 8. RMS bunch length sensitivity to bunch arrival time error (with respect to RF phase). The solid-RED line is with X-band RF OFF and the dashed-BLUE is with X-band RF at 18 MV (1 psec ≈ 1° S-band).

5 Wakefields and Aperture Limits

At an RF gradient of 40 MV/m, which is well below NLC requirements of 70 MV/m, an X-band section length of $L \approx 0.6$ m provides up to 24 MV. The mean iris radius typical for the NLC X-band structures is 4.7 mm with a 8.75-mm cell length, resulting in a mean transverse wakefield amplitude over a 1-mm rms bunch length of $\langle W_x \rangle \approx 7{\times}10^{16}$ V/C/m^2. The transverse emittance dilution for a short, misaligned structure, is approximately given by

$$\frac{\varepsilon}{\varepsilon_0} \approx \sqrt{1+\left(\frac{\pi r_e}{Z_0 c}\right)^2 \frac{N^2 \langle W_x \rangle^2 L^2 \beta}{\varepsilon_N \gamma} \Delta x^2}\ , \tag{12}$$

where r_e is the classical electron radius, Z_0 free-space impedance, c speed of light, N bunch population (6.2×10^9), β mean beta function in the structure (~5 m), ε_N normalized transverse emittance (1 μm), γ mean beam energy in structure in units of electron rest mass (260 MeV/mc^2), and Δx the misalignment. For the LCLS parameters (in parenthesis), the misalignment tolerance is $|\Delta x| < 200$ μm for $|\Delta\varepsilon/\varepsilon_0| < 8\%$. This is dominantly a linear time-correlated emittance growth and can also be corrected.

Finally, the physical aperture of the X-band iris is about half that of the S-band structures ($r_x \approx 4.7$ mm versus $r_s \approx 11.6$ mm) and may present an aperture limit or wakefield problem for high-charge, non-LCLS beams which are accelerated in the SLAC linac. For a high-charge, high-energy, non-LCLS beam with $N \approx 4\times10^{10}$, $\gamma \approx 25$ GeV/mc^2, $\beta \approx 50$ m, $\varepsilon_N \approx 5$ μm, the single bunch emittance growth is still just 8% at $\Delta x \approx 200$ μm. In this case, even for $\varepsilon_N \approx 50$ μm, the X-band structure allows a ± 20-σ aperture, which is about half the clearance of LCLS beams (± 45-σ aperture).

6 Acknowledgements

We thank M. Borland and R. Li for various conversations which were important input leading to this harmonic RF compensation approach. We also recognize that a similar 3rd-harmonic compensation approach was independently suggested and studied at Boeing by D. Dowell et al. [4], and at DESY by K. Floettmann and P. Piot [5].

7 References

[1] LCLS Design Study Report, SLAC-R-521, (1998).

[2] R. Li, *Analysis And Simulation On The Enhancement Of The CSR Effects,* 20th International Linac Conference (Linac 2000), Monterey, California, Aug 2000.

[3] *TESLA Technical Design Report*, DESY 2001-011, March 2001.

[4] D. Dowell et al., *Magnetic Pulse Compression Using a Third Harmonic Linearizer*, Proceedings of the 1995 Particle Accelerator Conference, Dallas, TX, May 1995.

[5] K. Floettmann, P. Piot, *The TESLA X-FEL Injector*, Proceedings of the 2001 Particle Accelerator Conference, Chicago, IL, June 2001.

[6] P. Emma, *Bunch Compressor Options for the New TESLA Parameters*, Nov. 1998, DAPNIA/SEA-98-54.

[7] C. Limborg, private communication, November 2001.